

THE GENERATION OF UNSTRUCTURED BOUNDARY-CONFORMING MESHES OF HIGH-ORDER ELEMENTS

Joaquim Peiró, Spencer J. Sherwin and Sergio Giordana

*Department of Aeronautics, Imperial College of Science, Technology and Medicine,
Prince Consort Road, London SW7 2BY, United Kingdom*

SUMMARY: The ability to construct suitable computational meshes is currently a significant limiting factor in the development of compact high-order algorithms, such as spectral elements or p -type finite elements, in very complex geometries. This article discusses the generation of 3D unstructured meshes of high-order elements that conform to the boundary of the computational domain and presents strategies to alleviate the problem of generation of distorted elements with singular elemental mappings.

KEYWORDS: High-order mesh generation, hybrid meshing, curvature based adaption, high-order elements.

INTRODUCTION

High-order unstructured algorithms, such as spectral elements [8] or p -type finite elements [9], offer the potential of high accuracy if the solution is smooth and a well behaved mapping exists between the elements in the mesh and a standard region. The extension of high-order algorithms to three-dimensional problems has already been addressed in these references, but their implementation within three-dimensional mesh generation and CAD surface representation techniques has received little attention. The development of high-order algorithms in very complex geometries is currently limited by progress in methods for high-order mesh generation.

However the extension of standard unstructured mesh generation technology to high-order algorithms is not a trivial exercise. Complications arise due to the conflicting requirements to generate coarse meshes whilst maintaining good elemental properties in regions of high curvature. For instance, Fig. 1 shows a valid discretization of the computational domain using linear elements, but the corresponding high-order discretization is unacceptable since it contains elements with singular local to global mappings.

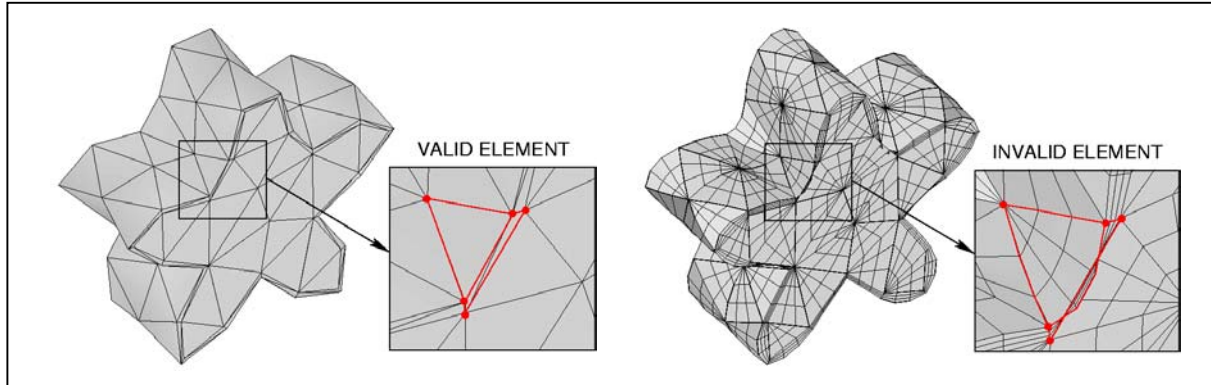


Fig. 1: The introduction of extra degrees of freedom in a valid mesh of linear elements (left) might lead to the appearance of invalid high-order elements (right).

In this paper we will discuss the method adopted for the generation of meshes of high-order elements with particular emphasis on the optimisation of the surface mesh generation, and will present techniques for avoiding the appearance of singular elements by refining the mesh according to the surface curvature. We will illustrate these techniques using the geometry depicted in Fig. 1. This is a cylinder of unit depth with a cross section generated as a sinusoidal perturbation of amplitude 0.8 to a circle of unit radius.

MESH GENERATION OF HIGH-ORDER ELEMENTS

The method adopted to generate an unstructured mesh of spectral/ hp elements, as originally presented in [5], is based on the post-processing of an unstructured mesh of linear elements and proceeds in three steps. The first step is to generate a discretisation of the boundary of the domain into triangular surface elements. The second step involves the transformation of this surface triangulation into high-order elements suitable for a spectral/ hp computation. Finally the interior volume is constructed using standard low-order mesh technology although more advanced techniques may generally be necessary as discussed in Dey et al. [1]. These steps are schematically represented in Fig. 2.

The geometry of the computational domain is defined through a boundary representation (B-Rep) where the domain is viewed as the interior region to a boundary composed by a set of faces on surfaces intersecting along curves where the edges of the boundary lie. This is shown in Fig. 2a. These curves and surfaces are described using standard techniques of computer-aided design (CAD) representation in terms of parametric curves and surfaces. Alternative representations such as implicit surfaces are currently being used in geometry reconstruction from images, particularly in medical applications. The application of the techniques presented here to implicit surfaces is discussed in reference [7].

The first stage of the high-order meshing is to generate a coarse linear surface triangulation, depicted in Fig. 2b, and then to modify these sub-domains into a *boundary conforming* mesh of high-order elements, shown in Fig. 2c, by splitting the sides and faces in a bottom-up fashion consistent with a B-Rep of the computational domain.

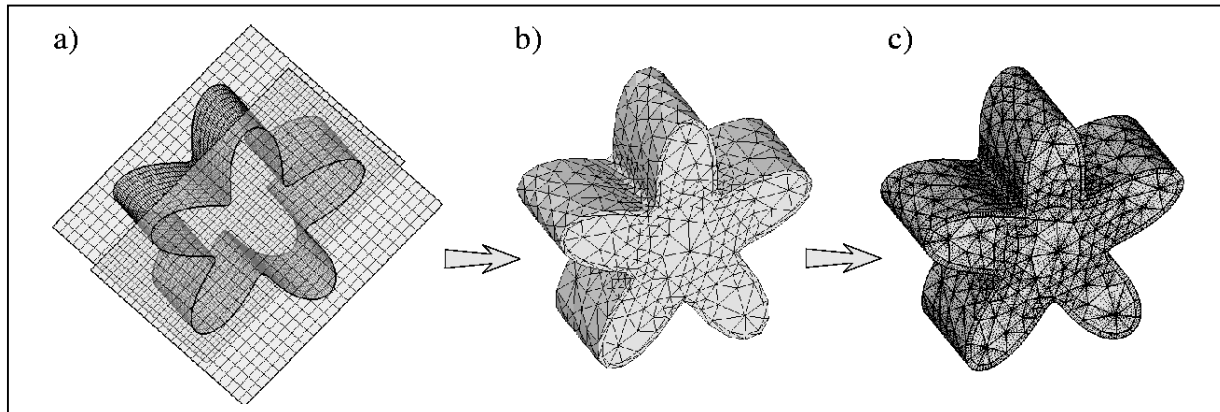


Fig. 2: Generation of a mesh of high-order elements: a) CAD boundary representation (B-Rep) of the domain, b) unstructured mesh of linear elements, and c) unstructured high-order mesh.

The generation of linear elements is achieved by using a modified advancing layers method in the near-wall regions and an advancing front technique in the rest of the domain as described in [6]. The meshes generated in this manner are employed in the modelling of viscous flows containing a boundary layer region near solid boundaries where the flow solution varies very rapidly. An unstructured boundary layer mesh can be constructed by extruding the surface triangulation in the wall normal direction. This produces a series of prismatic regions that can be subdivided into three tetrahedral elements. Such an approach is valid for meshes of linear elements and for high-order elements provided that the local surface is concave. However, in a locally convex region, the division of the prismatic regions into tetrahedral elements can lead to self intersecting elements as shown in Fig. 1. The obvious alternative is not to subdivide the prismatic region but apply a hybrid expansion. The computational domain then consists of an outer shell of prismatic regions surrounding an inner core of straight-sided tetrahedral elements as shown in Fig. 2b and 2c. Since the inner tetrahedral domain contains only straight-sided elements, the sub-domains are guaranteed to be valid if a valid low-order mesh has been constructed.

The generation of high-order elements therefore starts with a discretisation of the sides of the triangular surface elements into P points as required by a polynomial interpolation of degree $P-1$. There are two possible cases to consider. If the side belongs to a curve of the B-Rep, the intermediate $P-2$ points are placed along the length of the CAD curve where the edge lies. If the side is on a face of the B-Rep, then the intermediate points are positioned on the corresponding CAD surface. In both of these cases a point placement algorithm is required either within a parametric curve or surface. It is the generation of these points which we refer to as high-order mesh generation since this information is used to reconstruct a high-order numerical representation of the computational domain.

At present we complete the volume generation of linear elements using the modified advancing layer combined with an advancing front technique. The higher order surface information and the ability to deform element internally could be utilized during the process, as proposed in [1], but this has not been necessary here.

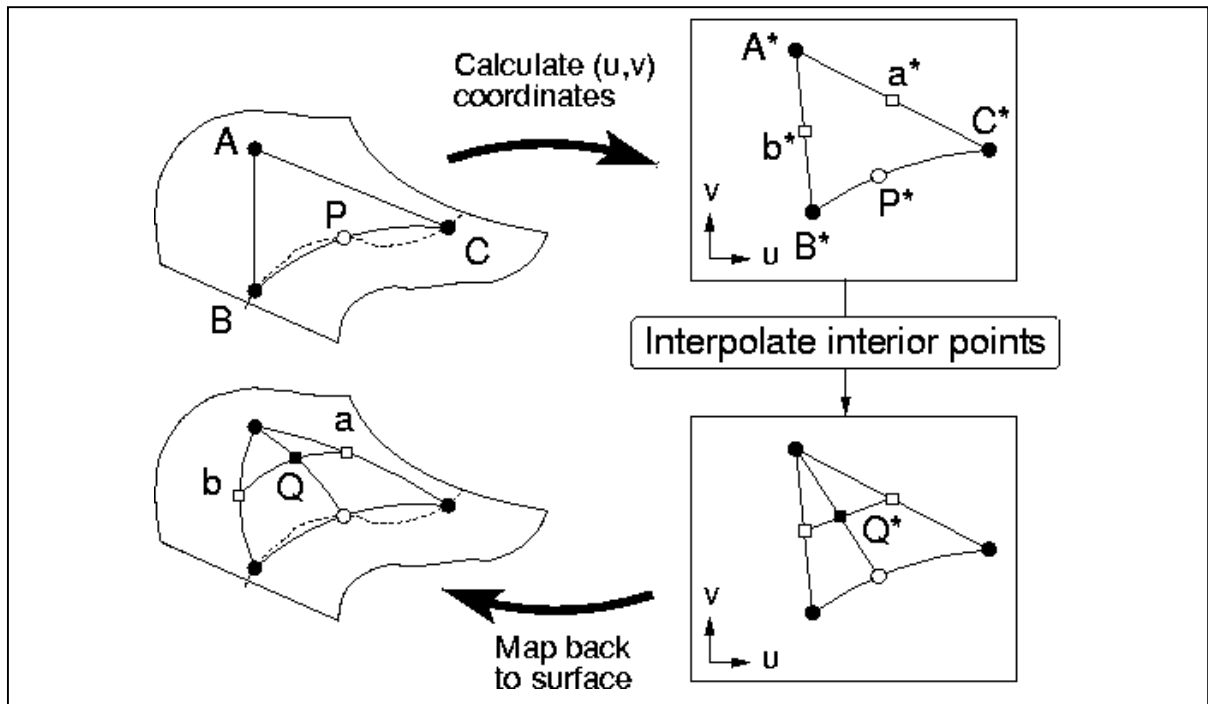


Fig. 3: Surface mesh subdivision procedure.

An important part of the high-order mesh generation process is the construction of high-order edges and faces on the CAD curves and surfaces of the B-Rep of the computational domain. To illustrate this process we consider the diagrammatic representation shown in Fig. 3. The starting point for the generation of a high-order representation of an elemental face belonging to a boundary is the definition of three vertices on a CAD surface. If an edge of the face lies on a CAD curve, its discretisation requires the placement of points along the CAD curve. Typically, a distribution based on a Gaussian quadrature is used. The shape of the other edges can be freely defined within the CAD surface. A computationally convenient approach is to use a linear interpolation between the parametric coordinates of the end points of the edge. The points in the interior of the face can be determined in a similar fashion by using, for example, a transfinite interpolation within the parametric plane. Finally the three-dimensional coordinates of the boundary points of the elemental face are obtained by mapping the calculated parametric coordinates onto the CAD surface.

The use of a transfinite interpolation between the discretised edges of triangles in the parametric space followed by a projection onto the surface does not take into account the metric information of the mapping between the physical and parametric space. For CAD surfaces represented by isometric mappings (i.e. those that preserve lengths) the above procedure produces reasonably good quality elements. In regions where the mapping is highly anisometric, such an approach can lead to very deformed mappings or, at worst, invalid elements. In the following section we propose a method to obtain an optimal distribution of mesh points through the minimisation of an appropriate function that represents the energy of the system.

OPTIMISING THE SURFACE APPROXIMATION

To address the problem of obtaining an optimal distribution of points, let us consider a quadrature with P integration points and associated normalised weights z_i ; $i=1,\dots,P$ ($-1 \leq z_i \leq 1$) in a one-dimensional interval $a \leq x \leq b$. It is known that the optimal positions x_i ; $i=1,\dots,P$ of the points are given by

$$x_i = a \left(\frac{1-z_i}{2} \right) + b \left(\frac{1+z_i}{2} \right); \quad i=1,\dots,P \quad (1)$$

which lead to an isometric mapping and therefore a constant Jacobian. An optimal distribution of integration points for curves is easily obtained by interpreting the coordinate x as the arc length of the curve. The implementation of this criterion using parametric CAD curves is relatively straightforward and amounts to finding the coordinates of a point in the curve that corresponds to the required length.

This procedure can be extended to elements with straight sides and faces by using a tensor-product of optimal distributions along coordinate lines. However, a different strategy is required to achieve such an optimal distribution for *curved* edges and faces as we need to account for the distortion introduced by the presence of curvature.

A parametric surface is defined as a transformation between a two-dimensional parametric space (u,v) and a three-dimensional space $\mathbf{r}(u,v) = [x(u,v), y(u,v), z(u,v)]$. Mesh generation is considerably simplified if performed in a parametric space. Therefore, as previously discussed, a computationally straightforward approach, illustrated in Fig. 3, is to approximate the element edge by a straight line in the parametric plane and to distribute the points along that line according to equation (1). A similar approach has been adopted in the work of Dey et al. [1]. However, as discussed previously, if the transformation $\mathbf{r}(u,v)$ is anisometric, this approach can lead to highly deformed or invalid elemental regions.

Optimal distribution of edge points

A more general procedure can be obtained by reformulating the problem of finding the optimal distribution of points as that of minimising the potential energy of a set of springs linking adjacent points. If the stiffness of a spring joining nodes i and $i+1$ is taken to be inversely proportional to the weight increment $z_{i+1} - z_i$, it is easily shown that the optimal distribution (1) is a minimum of the potential energy, denoted here by \mathfrak{F} , of such system of springs given by

$$\mathfrak{F}(x_2, \dots, x_{P-1}) = \sum_{i=1}^{P-1} \frac{(x_{i+1} - x_i)^2}{z_{i+1} - z_i}. \quad (2)$$

This approach, unlike equation (1), is directly applicable to curved edges and faces on surfaces. The implementation of this approach to edges on a parametric surface is slightly more involved. Since our parametric surface is defined in terms of the parametric coordinates $\mathbf{u} = (u,v)$, we recast the cost function as

$$\mathfrak{F}_e(\mathbf{u}_2, \dots, \mathbf{u}_{P-1}) = \sum_{i=1}^{P-1} \frac{\left\| \mathbf{r}(u_{i+1}, v_{i+1}) - \mathbf{r}(u_i, v_i) \right\|^2}{z_{i+1} - z_i}. \quad (3)$$

In this two-dimensional minimisation procedure, the end points of the edge are fixed and the curve defining the edge is free to move in the parametric surface. This minimisation procedure is also *non-linear* since it involves the mapping $\mathbf{r}(u,v)$ between the physical coordinates and the parametric plane. The main advantage of this approach with respect to the transfinite interpolation is that the optimal solution will tend to a geodesic of the surface between the two end points and the distribution of points along the geodesic will also tend towards the optimal quadrature distribution.

The cost function (3) can also be easily adapted to deal with the discretization of curved edges defined as a function of a single parameter u . The minimisation clearly does not alter the length of the curve and it will position the points in accordance with the quadrature distribution (1).

Optimal distribution of face points

The spring network analogy can also be applied to find the location of interior points within a curved elemental face. Assuming that a good distribution of points is known for a planar straight sided triangle, we can ask what is the set of stiffnesses k in a network of springs that will produce the same distribution of points as its equilibrium position?

Here we assume a tensor-product distribution of quadrature points with P points in each direction. The positions of the quadrature points in the parametric space are denoted by $\mathbf{u}_{i,j} = (u_{i,j}, v_{i,j})$; $i, j = 1, \dots, P$ and the optimal distribution of the interior points is obtained by minimizing the potential energy of the system defined as

$$\begin{aligned} \mathfrak{S}_f(\mathbf{u}_{2,2}, \dots, \mathbf{u}_{i,j}, \dots, \mathbf{u}_{P-1,P-1}) = & \sum_{j=2}^{P-1} \sum_{i=1}^{P-1} \frac{\left\| \mathbf{r}(u_{i+1,j}, v_{i+1,j}) - \mathbf{r}(u_{i,j}, v_{i,j}) \right\|^2}{z_{i+1}^{(1)} - z_i^{(1)}} + \\ & \sum_{i=2}^{P-1} \sum_{j=1}^{P-1} \frac{\left\| \mathbf{r}(u_{i,j+1}, v_{i,j+1}) - \mathbf{r}(u_{i,j}, v_{i,j}) \right\|^2}{z_{j+1}^{(2)} - z_j^{(2)}}. \end{aligned} \quad (4)$$

The symbols $z_i^{(1)}$ and $z_j^{(2)}$ denote the quadrature weights in the i and j directions respectively. A slightly modified version of this method could also be applied to the problem of finding the optimal position of the interior points within a curved element. Although we have assumed a tensor-product distribution of the points defining the polynomial interpolation within the element, any distribution of points can be minimised in this fashion by an appropriate choice of the spring network. The reader is referred to reference [8] for further details.

To illustrate the surface mesh generation methodology, we consider the generation of a tetrahedral p -type mesh of fifth order polynomial within a simple cubic computational domain $0 \leq x, y, z \leq 10$. The faces of the cube are located on tensor-product surfaces defined by an anisometric mapping shown in Fig. 4a). The spacing varies linearly with a value of $\delta = 0.1$ at the boundary and $\delta = 2.1$ at the centre of the faces. The anisometry of the mapping is due to the fact that the unevenly spaced network of lines depicted in Fig. 4a) is obtained as the image of a network of coordinate lines $u = \text{const.}$ and $v = \text{const.}$ in the parametric plane which are uniformly spaced with $\Delta u = \Delta v = 1$ as depicted in Fig. 4d. The curve definition of the edges representing the intersection between each of the faces was taken to be isometric.

A standard h -type unstructured mesh generation process was used to construct a coarse mesh with 66 elements. Although the p -type elements can easily be constructed on a planar surface by a linear interpolation between the vertices, we have chosen to reconstruct the surface elements using the parametric definition of the surface as required for a non-planar surface. Therefore we know that the optimal solution for this geometry is a linear distribution of points between the vertices according to the quadrature distribution given by equation (1).

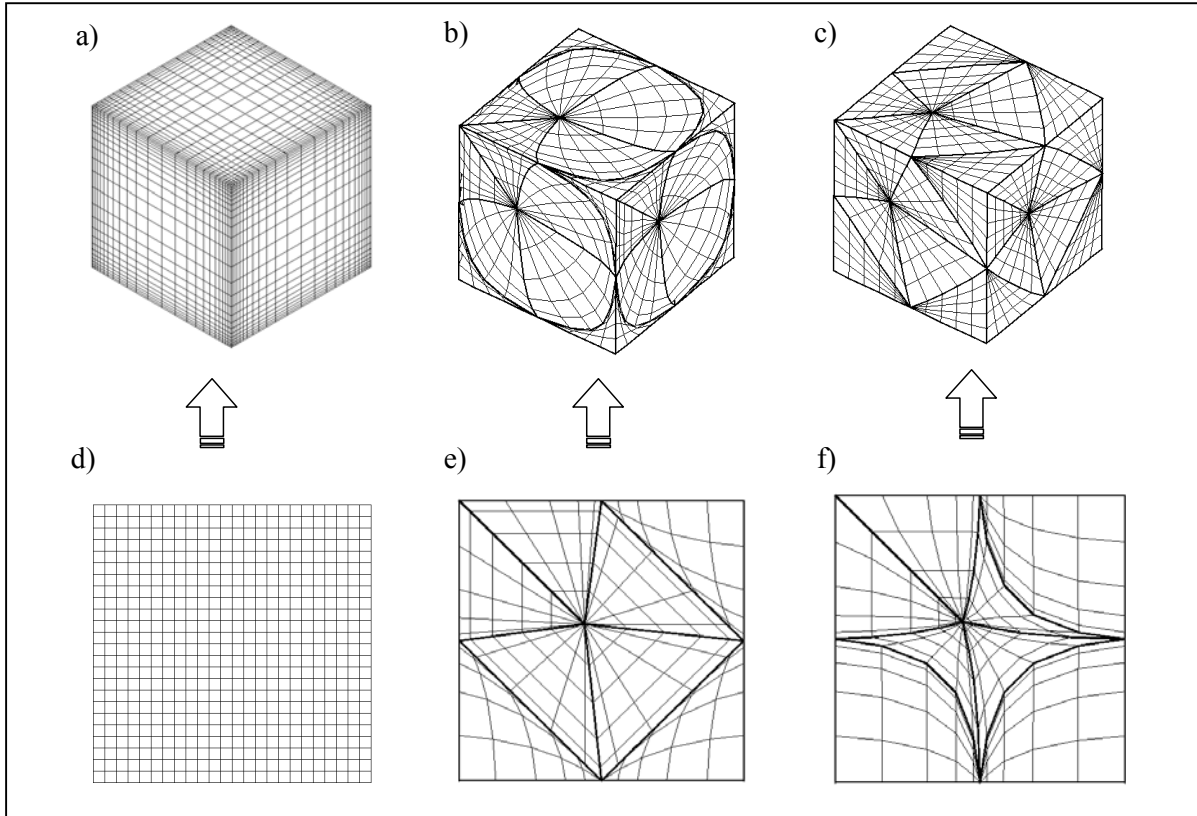


Fig. 4: Influence of surface mapping on the p -type generation procedure. a) Anisometric CAD description. The corresponding representation in the parametric space is depicted in Fig. 4d. b) High-order mesh using a transfinite interpolation in the parametric space represented in Fig. 4e. c) High-order mesh using an optimised point placement in the parametric space as shown in Fig. 4f.

However if we apply the optimisation procedure based on the spring analogy, we obtain the surface mesh shown in Fig. 4c which produces a fit very close to a linear mapping between the vertices. A natural consequence of obtaining a good physical surface distribution is that the parametric distribution becomes very distorted as shown in figure Fig. 4f. Mesh distortion in the physical space has a strong influence in the accuracy of the numerical solution. Results presented in reference [8] for an elliptic problem have shown that the optimized method leads to improved rates of convergence, as the mesh size is decreased, with respect to the transfinite interpolation in the parametric space.

CURVATURE BASED DISCRETIZATION

Curvature based refinement in which the mesh size is obtained as a function of the curvature has been proposed, see for instance [3], as a way to obtain an accurate piecewise linear approximation of a curved surface. Following the notation of Fig. 5a, the curve is locally

approximated by a circle of radius R , the radius of curvature. We assume that the mesh spacing can be represented by a chord of length c in the circle. Denoting the maximum distance between the chord and the circle by t , we restrict its value, as suggested in [3], to $t \leq \varepsilon R$, where ε is a user defined tolerance. The mesh spacing, δ , can now be obtained as a function of R and ε as

$$\delta \approx c \leq 2R\sqrt{\varepsilon(2-\varepsilon)} \quad (5)$$

As a guide, a value of $\varepsilon = 0.01$ results in the division of a circle into 26 segments.

The use of this technique enhances the quality of the high-order meshes generated from linear tetrahedral and prismatic meshes [8]. However, this criterion on its own is not sufficient to guarantee validity of all high-order elements as it does not account for the possible intersection of the boundary sides and faces with those on the interior. Here we propose an alternative method more suitable for the discretization of boundary layers.

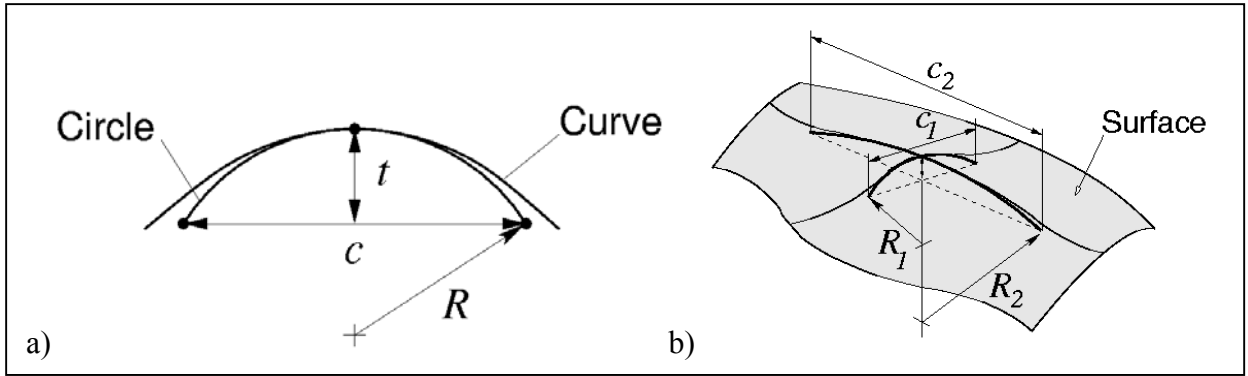


Fig. 5: Notation for curvature calculation: a) curves, and b) surfaces.

In the modelling of viscous flows, the value of δ is usually prescribed to achieve a certain boundary layer resolution. Following the notation in Fig. 6, the value of c is therefore chosen to guarantee that the osculating circle representing the curve does not intersect the interior sides of the elements, i.e. $\theta \leq 90^\circ$ for the triangular element in Fig. 6a. The value of c , which should be considered as a maximum mesh spacing, can now be obtained as a function of R and δ . Its value c_t for triangular elements is

$$c_t \leq R\sqrt{\frac{2\delta}{R+\delta}} \quad (6)$$

and the corresponding value c_q for quadrilateral elements is

$$c_q \leq \frac{2R\delta}{R+\delta} \sqrt{1 + \frac{2R}{\delta}}, \quad (7)$$

where the boundary displacement is assumed to be the same on either side of the rectangle. It is interesting to notice that, for a given δ , the quadratic element allows for a mesh spacing c_q which is about twice the value of spacing c_t for the triangular element.

The extension of the curvature refinement method to surfaces is straightforward. The refinement criteria given by formulas (5), (6) and (7) is used for the two principal directions and the corresponding mesh spacings, c_1 and c_2 in figure Fig. 5b, are calculated from the values of the principal curvatures R_1 and R_2 . Expressions for the curvature of curves and surfaces can be found in reference [2].

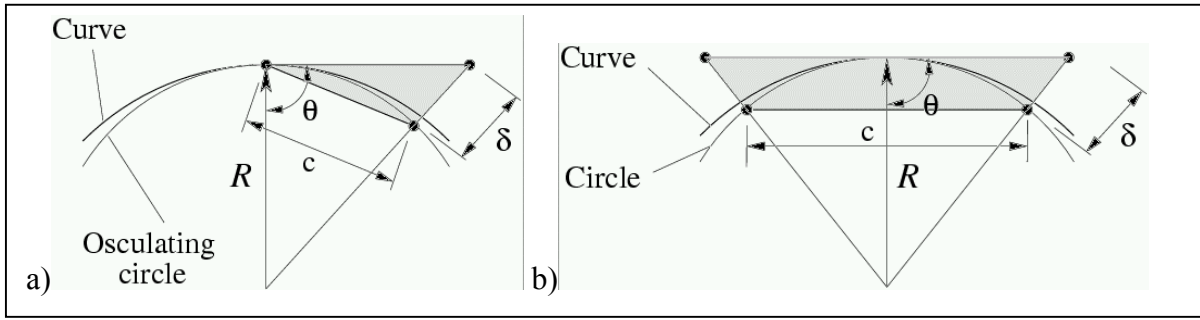


Fig. 6: Notation for mesh spacing calculation on curves: a) triangular element and b) quadrilateral element.

An example of a hybrid mesh generated for the geometry previously considered in Fig.1 and using the criterion given by equation (5), is shown in Fig. 7a. The value of ε in equation (5) has been chosen to be the largest one that produces a high-order mesh without singular elements. The final mesh contains 2388 high-order elements with fifth order ($P=5$) polynomial interpolation. Fig. 7b shows the surface plot variation of the quality of the mesh represented by the index Q_{3D} defined as the ratio between the global minimum and maximum values of the Jacobian determinant of the mapping, J_q , over the discrete set of quadrature points $q = 1, \dots, N_q$, this is

$$Q_{3D} = \frac{\min(J_q)}{\max(J_q)}, \quad q = 1, \dots, N_q. \quad (8)$$

This mesh has a minimum value of $Q_{3D} = 0.15$ corresponding to a factor of 7 variation in the elemental Jacobian.

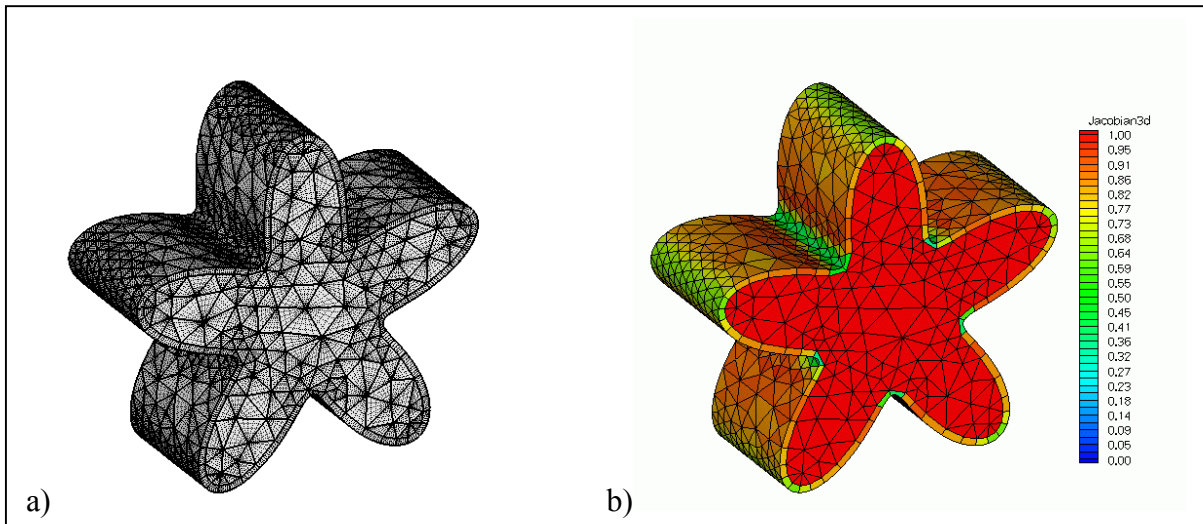


Fig. 7: Curvature based mesh refinement for prismatic elements according to equation (5): a) high-order mesh, and b) distribution of the mesh quality index Q_{3D} .

The application of the refinement criterion (7) to the same geometry leads to the mesh and distribution of quality index depicted in Fig. 8. The mesh contains now 1692 elements with a larger number of elements with an index Q_{3D} close to one than the previous mesh (Fig. 7).

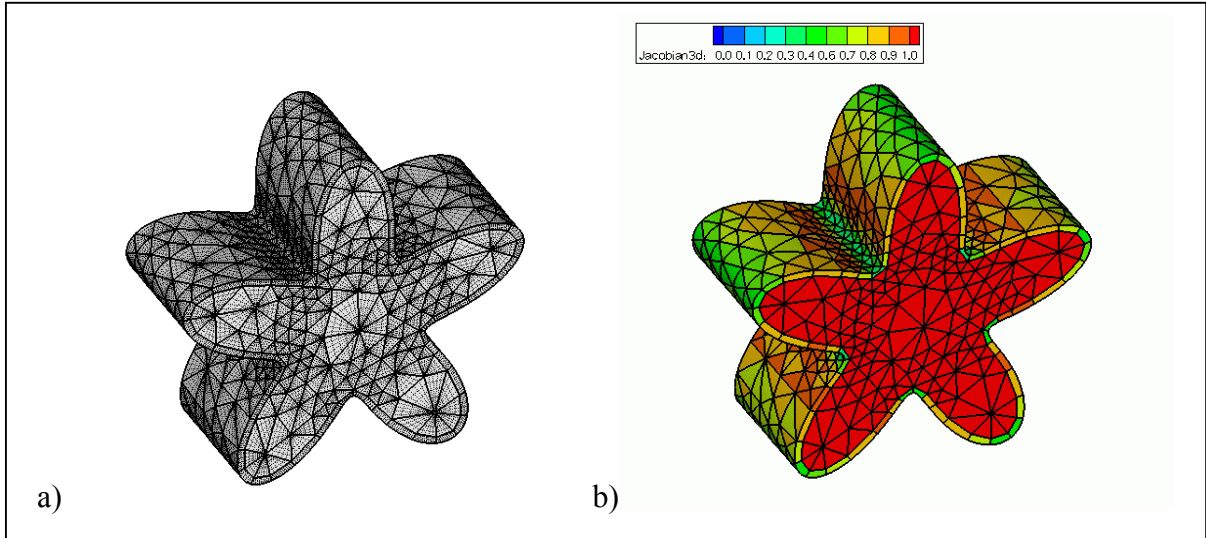


Fig. 8: Curvature based mesh refinement for prismatic elements according to equation (7): a) high-order mesh, and b) distribution of mesh quality index Q_{3D} .

However, the refinement applied here does not account for the sign of the surface curvature and these curvature based criteria are too restrictive to ensure element validity in those regions where the domain is locally convex. For a *convex* region, the less restrictive criterion

$$\delta \leq R \quad (9)$$

suffices to guarantee element validity. This is highlighted in Fig. 9 where the refinement criterion (7) has been selectively applied to concave regions only. The result is a valid mesh with fewer elements (1424) and a similar distribution of the quality index Q_{3D} .

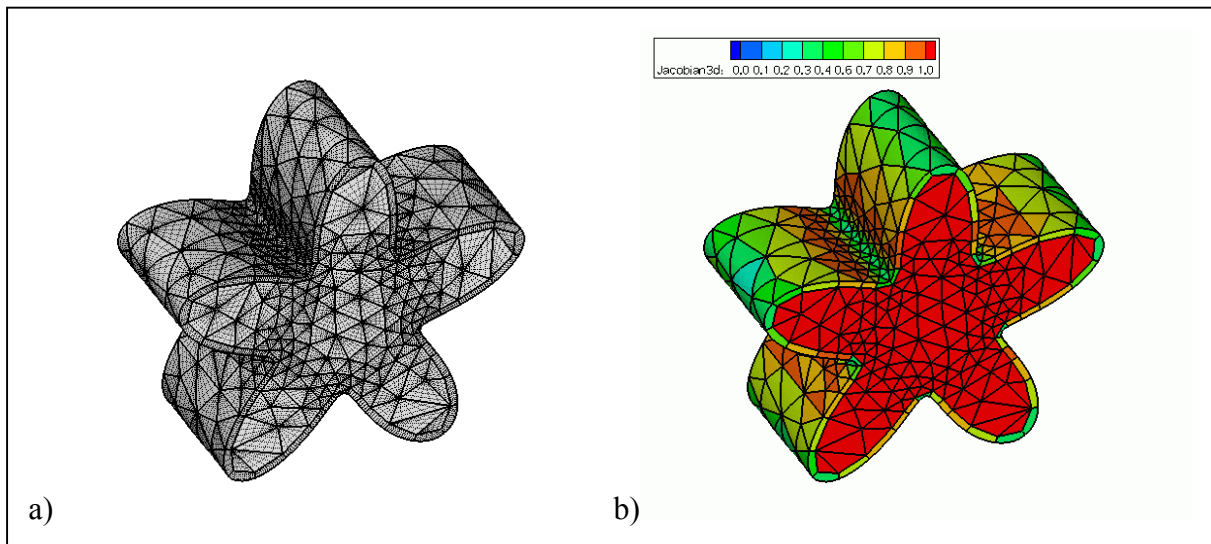


Fig. 9: Selective curvature refinement: The criteria (7) is applied to concave regions. Concave regions are applied the less restrictive requirement (9).

CONCLUSIONS

In this paper we have presented a set of strategies to generate unstructured meshes of valid high-order elements. These represent a step forward towards the elusive target of consistently generating valid computational meshes for complex geometries without user intervention. The starting point is a coarse mesh of linear elements that can be generated by traditional unstructured mesh generation techniques. However, the subdivision of this mesh into a boundary conforming mesh of high-order elements requires careful handling due to the distortion that non-planar surfaces might introduce.

We have presented methods for generating a hybrid discretisation using prismatic and tetrahedral elements, together with an approach for generating optimal surface discretisations for high-order elements that accounts for surface curvature. This generation process minimises the element distortion due to the surface curvature based refinement by searching for the shortest geodesic line between two points whilst maintaining a Gaussian quadrature distribution. Finally the use of curvature-based refinement has proven to be a very useful tool to produce valid high-order meshes with fewer elements.

ACKNOWLEDGEMENTS

The authors would like to acknowledge support from the Smiths' Charity, the Bupa foundation, the Heartbeat charity and the Clothworkers' Foundation. The Imperial College centres for Biomedical Visualization and Parallel Computing provided computational resources.

REFERENCES

1. Dey, S., Shephard, M.S. and Flaherty, J.E., "Geometry representation issues associated with p -version finite element computations", *Comp. Meth. Appl. Mech. Engng.*, **150**, 1997, pp. 39-55.
2. Do Carmo, M.P., "Differential Geometry of Curves and Surfaces", Prentice-Hall, 1976.
3. P. Frey and P-L. George, "Maillages", Editions Hermes, 1999.
4. Karniadakis, G.E. and Sherwin, S.J., "Spectral/ hp Element Methods for CFD", Oxford University Press, 1999.
5. Peiró, J., Shah, O., Doorly, D. J., Sherwin, S. J. and Caro C.G., "Unstructured Viscous Mesh Generation for Haemodynamic Flow Simulation Using High-Order Spectral Elements", *Proc. 6th International Conference on Numerical Grid Generation in Computational Field Simulations*, Greenwich, U.K., 1998, pp. 457-466.
6. Peiró, J. and Sayma, A.I., "A 3-D Unstructured Multigrid Navier-Stokes Solver", *Numerical Methods for Fluid Dynamics V*, Morton, K.W. and Baines, M.J., Eds., Oxford University Press, 1995.
7. Peiró, J., Giordana, S., Griffith, C. and Sherwin, S.J., "High-Order Algorithms for Vascular Flow Modelling", Accepted for publication in *Int. J. Numer. Meth. Fluids*, 2002.
8. Sherwin, S.J., and Peiró, J., "Mesh Generation in Curvilinear Domains Using High-Order Elements", *Int. J. Numer. Meth. Engng.*, **53**, 2002, pp. 207-223.
9. Szabó, B. and Babuška, I., "Finite Element Analysis", Wiley, 1991.